

### 2.4.9 Cap-Yield (Cysoil) Model

The double-yield model (see [Section 2.4.6](#)) is a shear and volumetric hardening/softening model for the simulation of soil behavior. One flexible feature of the model is the capability for adding user-defined hardening/softening laws, which are then communicated to the model by means of tables. As mentioned by Davis and Sepulvadurai (2002), the general concept of hardening is very useful whenever there is a need for model responses that are more detailed than is possible with perfect plasticity. In particular, a closed yield surface would be almost useless without volumetric (cap) hardening.

The motivation for closing the yield surface by a cap on the mean stress axis is to permit plastic behavior in response to an isotropic stress increase. This plasticity effect accounts for grain crushing and rearrangement, and is particular to soils. In the double-yield model, the cap is a plane, normal to the mean stress axis in stress space. The impact of this particular shape on the coefficient of lateral earth pressure,  $K_0$ , as predicted by the model in uniaxial compression tests has been considered to be somewhat restrictive by some users. The Cysoil model is a modification of the double-yield model that addresses this issue by accounting for a cap with an elliptic shape in the  $(p', q)$  plane. The ratio of axes of the ellipse,  $\alpha$ , determines the value of  $K_0$ , and is a material property for the model, which can be chosen to match a known value in uniaxial compression.

In addition, soils, when subjected to deviatoric loading, usually exhibit a decrease in stiffness accompanied by irreversible deformation. In most cases, the plot of deviatoric stress versus axial strain obtained in a drained triaxial test may be approximated by a hyperbola. This feature has been used by Duncan and Chang (1970) to formulate their well-known “hyperbolic soil” model. (See ‘408S0038’ in the **User’s Guide**.) The hyperbolic soil model of Duncan and Chang is a non-linear elastic model that has been shown to exhibit some drawbacks. These drawbacks include, for example, difficulty in detecting and characterizing unloading/reloading, and, in specific cases, producing a non-physical bulk-modulus value that can lead to an erroneous energy generation in the model. Because the Cysoil model is formulated in the theory of hardening plasticity, it allows for an alternative expression of the hyperbolic behavior (based on friction hardening), which is capable of addressing some of these problems.

When tested under drained triaxial conditions, soils generally exhibit shear induced volume changes that are strongly dependent on soil density. Typically, there is a tendency for the soil to contract under small shear strains, and to dilate under larger strains, unless it is very loose (Byrne et al. 2003). In particular, when fluid fills the pores, it is this tendency of the soil skeleton to contract and dilate that controls its liquefaction response. Also, the shear stress - shear strain response of loose soil may exhibit a softening response under undrained conditions. It is the existence of a peak in shear strength, which may lead to instability (static liquefaction) during a monotonic load-controlled process (Boukpeti 2001). Shear induced volume changes can be accounted for in the Cysoil model by means of a dilation hardening/softening law.

The Cysoil model is a strain-hardening constitutive model characterized by a frictional Mohr-Coulomb shear envelope (zero cohesion), and an elliptic volumetric cap with ratio of axes, defined by a shape parameter  $\alpha$ . For zero cohesion, the double-yield model, with its planar volumetric cap, is obtained as a special case of the Cysoil formulation by assuming a value of  $\alpha$  large compared to 1. The basic model is described in the following sections.

The basic Cysoil model behavior can be enhanced using three types of hardening laws: a cap-hardening law, to capture the volumetric power law behavior observed in isotropic compaction tests, a friction-hardening law, to reproduce the hyperbolic stress-strain law behavior observed in drained triaxial tests, and a compaction/dilation law to model irrecoverable volumetric strain taking place as a result of soil shearing. This customizing of the Cysoil model is discussed in [Section 2.4.9.3](#).

#### 2.4.9.1 Incremental Elastic Law

The elastic behavior is expressed using Hooke's law. The incremental expression of the law in terms of principal stress and strain\* has the form:

$$\begin{aligned}\Delta\sigma'_1 &= \alpha_1 \Delta e_1^e + \alpha_2 (\Delta e_2^e + \Delta e_3^e) \\ \Delta\sigma'_2 &= \alpha_1 \Delta e_2^e + \alpha_2 (\Delta e_1^e + \Delta e_3^e) \\ \Delta\sigma'_3 &= \alpha_1 \Delta e_3^e + \alpha_2 (\Delta e_1^e + \Delta e_2^e)\end{aligned}\tag{2.243}$$

where  $\alpha_1 = K^e + 4G^e/3$ ,  $\alpha_2 = K^e - 2G^e/3$ , and  $K^e$  and  $G^e$  are current, tangent elastic bulk and shear modulus, respectively. Some useful relations between  $K^e$ ,  $G^e$ , Young modulus,  $E^e$  and Poisson's ratio,  $\nu$  are listed below for reference:

$$K^e = \frac{E^e}{3(1-2\nu)} \quad G^e = \frac{E^e}{2(1+\nu)}\tag{2.244}$$

$$\frac{K^e}{G^e} = \frac{2(1+\nu)}{3(1-2\nu)}$$

---

\* Principal stress and strain components, represented by the symbol  $\sigma_i$  and  $e_i$  ( $i = 1,3$ ), respectively, are positive in extension. Also, effective stresses are denoted by a prime. The principal effective stresses are  $\sigma'_1, \sigma'_2, \sigma'_3$  and by convention  $\sigma'_1 < \sigma'_2 < \sigma'_3$  (i.e.  $\sigma'_1$  is the most compressive stress).

### 2.4.9.2 Yield and Potential Functions

*Shear Yield Criterion and Flow Rule* — Shear yielding is defined by a Mohr-Coulomb criterion. The yield envelope is expressed, in a form consistent with the cap formulation, as follows:

$$f = Mp' - q \quad (2.245)$$

where  $p'$  is the mean effective stress,  $p' = -(\sigma'_1 + \sigma'_1 + \sigma'_1) / 3$ ,  $q$  is a measure of shear stress, defined as:

$$q = -[\sigma'_1 + (\delta - 1)\sigma'_2 - \delta\sigma'_3] \quad (2.246)$$

Also, in these equations,  $\delta = (3 + \sin \phi_m) / (3 - \sin \phi_m)$ , and  $M = 6 \sin \phi_m / (3 - \sin \phi_m)$ .

In the *FLAC* formulation, the mobilized friction angle,  $\phi_m$ , is given in terms of plastic shear strain measure,  $\gamma^P$ , by means of a user-defined table. If no table is provided, it is assumed that friction is constant and equal to the input value of the friction property. Also, plastic shear strain,  $\gamma^P$ , is measured by a hardening parameter, whose incremental form is the second invariant of the incremental plastic deviatoric strain tensor (see [Section 2.4.4.1](#)).

The potential function is non-associated, and has the form:

$$g = M^* p' - q^* \quad (2.247)$$

where

$$q^* = [\sigma'_1 + (\delta^* - 1)\sigma'_2 - \delta^*\sigma'_3] \quad (2.248)$$

In these equations,  $\delta^* = (3 + \sin \psi_m) / (3 - \sin \psi_m)$ , and  $M^* = 6 \sin \psi_m / (3 - \sin \psi_m)$ . Also, the mobilized dilatancy angle,  $\psi_m$ , is given in terms of plastic shear strain,  $\gamma^P$ , by means of a user-defined table. If no table is provided, it is assumed that dilation is constant and equal to the input value of dilation property.

*Volumetric Cap Criterion and Flow Rule* — Yielding on the cap is associated; the criterion is:

$$f_c = \frac{q^2}{\alpha^2} + p'^2 - p_c^2 \quad (2.249)$$

where  $\alpha$  is a dimensionless parameter, defining the shape of the elliptical cap in the  $(p', q)$  plane, and  $p_c$  is cap pressure. The hardening curve relating cap pressure,  $p_c$ , to cap plastic volumetric

strain,  $e^p$ , is provided by means of a user-defined table. If no table is provided,  $p_c$  is assumed to be constant, and equal to the input value of cap pressure property.

Similar to the double-yield model, the Cysoil model uses a simple rule whereby the incremental elastic stiffness,  $K^e$  is proportional to the current incremental plastic stiffness  $H = dp_c/de^p$ . The factor of proportionality is a constant,  $R$ . The current value of elastic shear modulus,  $G^e$ , is derived assuming a constant Poisson's ratio, using the input upper bound values of shear and bulk modulus.

*Hardening Parameters* — The evolution parameters for shear and cap yielding are independent. The parameter for shear yielding,  $\gamma^p$ , is defined incrementally as

$$\Delta\gamma^p = \left\{ \frac{1}{2} \left( (\Delta e_1^{dp})^2 + (\Delta e_2^{dp})^2 + (\Delta e_3^{dp})^2 \right) \right\}^{\frac{1}{2}} \quad (2.250)$$

where  $\Delta e_j^{dp}$ ,  $j = 1, 3$  are the principal deviatoric plastic shear strain increments.

The evolution parameter for cap yielding is the modulus of plastic volumetric strain,  $e^p = e_1^p + e_2^p + e_3^p$ , where  $e_i^p$ ,  $i = 1, 3$  are the (accumulated increments of) principal plastic strains from yielding on the cap.

#### 2.4.9.3 Customizing the Cysoil Model

*Cap Hardening* — Soil stiffness usually increases in a non-linear fashion as a function of isotropic pressure. A cap-hardening table is used to specify a power law behavior. In most experimental cases, soil volumetric behavior in an isotropic compaction test can be captured by a power law of the form:

$$\frac{dp'}{de} = K_{ref}^{iso} \left( \frac{p'}{p_{ref}} \right)^m \quad (2.251)$$

where  $e$  is (minus) volumetric strain,  $K_{ref}^{iso}$  is the slope of the laboratory curve for  $p'$  versus  $e$  at reference effective pressure,  $p_{ref}$ , and  $m$  is a constant ( $m < 1$ ). A typical graph, representative of this law is sketched, with a small unloading excursion, in [Figure 2.39](#).

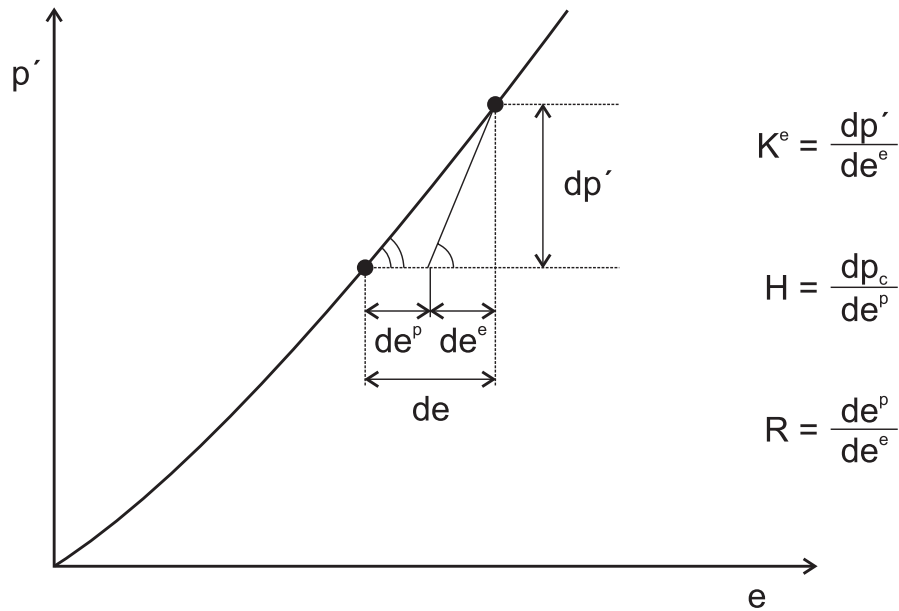


**Figure 2.39** *Isotropic consolidation test: pressure versus volumetric strain*

For input into the Cysoil model, a relation between cap pressure,  $p_c$ , and plastic volumetric strain,  $e^p$ , is required. This relation can be obtained from the following considerations. For isotropic compression  $dp' = dp_c$ , and we can write:

$$\frac{dp_c}{de^p} = \frac{de}{de^p} \frac{dp'}{de} \quad (2.252)$$

Now, the total strain increment has elastic and plastic contributions:  $de = de^e + de^p$ . Substitution of this expression for  $de$  in Eq. (2.252) gives:

$$\frac{dp_c}{de^p} = \frac{de^e + de^p}{de^p} \frac{dp'}{de} \quad (2.253)$$

The Cysoil model assumes that the ratio of elastic modulus  $K^e$  to hardening modulus  $H$  is equal to a constant,  $R = K^e / H$ , where, by definition,  $K^e = dp' / de^e$ , and  $H = dp_c / de^p$ . For isotropic compression  $dp' = dp_c$ , and we can write:

$$R = \frac{de^p}{de^e} \quad (2.254)$$

Finally, using Eq. (2.254) in Eq. (2.253) gives, after some manipulation:

$$\frac{dp_c}{de^p} = \frac{1+R}{R} \frac{dp'}{de} \quad (2.255)$$

After substitution of Eq. (2.251) in Eq. (2.255), we obtain:

$$\frac{dp_c}{de^p} = \frac{1+R}{R} K_{ref}^{iso} \left( \frac{p'}{p_{ref}} \right)^m \quad (2.256)$$

Integration of this expression gives, with  $p_c = 0$  at  $e^p = 0$ :

$$p_c = p_{ref} \left[ (1-m) \frac{1+R}{R} \frac{K_{ref}^{iso}}{p_{ref}} e^p \right]^{\frac{1}{1-m}} \quad (2.257)$$

This formula is used to generate the input table of  $p_c$  in terms of  $e^p$ . The law has 4 parameters:  $K_{ref}^{iso}$ ,  $p_{ref}$ ,  $m$  and  $R$ . Note that, since the Cysoil model assumes that  $K^e = R \times dp_c/de^p$ , by virtue of Eq. (2.256), the equation for the elastic bulk modulus is:

$$K^e = (1+R) K_{ref}^{iso} \left( \frac{p'}{p_{ref}} \right)^m \quad (2.258)$$

*Friction Hardening* — For most soils, the plot of deviatoric stress versus axial strain obtained in a drained triaxial test may be approximated by a hyperbola. The model is supplemented by a friction, strain-hardening table to capture this hyperbolic behavior. For friction-hardening behavior, we adopt the following, (hyperbolic) incremental law, similar to the one implemented in the UBCSAND model (Byrne et al. 2003):

$$d(\sin \phi_m) = \frac{G^p}{p'} d(\gamma^p) \quad (2.259)$$

where  $p'$  is effective pressure, and the plastic shear modulus  $G^p$  is given by

$$G^p = \beta G^e \left( 1 - \frac{\sin \phi_m}{\sin \phi_f} R_f \right)^2 \quad : \phi_m \leq \phi_f \quad (2.260)$$

In this formula,  $G^e$  is the elastic tangent shear modulus,  $\phi_f$  is the ultimate friction angle,  $R_f$  (the failure ratio) is a constant, smaller than 1 (0.9 in most cases) used to assign a lower bound for  $G^p$ , and  $\beta$  is a calibration factor.

The elastic tangent shear modulus is a function of  $p'$ , and we have

$$G^e = G_{ref}^e \left( \frac{p'}{p_{ref}} \right)^m \quad (2.261)$$

where  $G_{ref}^e$  is elastic tangent shear modulus at reference effective pressure  $p^{ref}$ , and  $m$  is a constant ( $m \leq 1$ ), taken as 1 for this discussion. After substitution of Eq. (2.261) in Eq. (2.260), the resulting expression in Eq. (2.259), and rearranging terms, we obtain

$$d(\gamma^p) = \frac{p_{ref}}{G_{ref}^e} \left( \frac{p'}{p_{ref}} \right)^{1-m} \frac{d(\sin \phi_m)}{\left( 1 - \frac{\sin \phi_m}{\sin \phi_f} R_f \right)^2} \quad (2.262)$$

Using that  $\phi_m = 0$  at  $\gamma^p = 0$ , integration of this expression gives

$$\gamma^p = \frac{p_{ref}}{G_{ref}^e} \left( \frac{p'}{p_{ref}} \right)^{1-m} \frac{\sin \phi_f}{R_f} \left[ \frac{1}{1 - \frac{\sin \phi_m}{\sin \phi_f} R_f} - 1 \right] \quad (2.263)$$

For  $m = 1$ , the hardening law simplifies to

$$\gamma^p = \frac{p_{ref}}{G_{ref}^e} \frac{\sin \phi_f}{R_f} \left[ \frac{1}{1 - \frac{\sin \phi_m}{\sin \phi_f} R_f} - 1 \right] \quad (2.264)$$

This expression is used to generate the model input table of friction in terms of plastic shear strain. As demonstrated in the example below, the use of this hardening law for modeling primary loading in a triaxial test will produce a hyperbolic curve of deviatoric stress versus axial strain. The law has 5 parameters:  $G_{ref}^e$ ,  $p_{ref}$ ,  $R_f$ ,  $\phi_f$  and  $\beta$ .

*Dilation Hardening* —A certain amount of irrecoverable volumetric strain,  $e^p$ , is expected to take place as a result of soil shearing. Also, under small (monotonic or cyclic) shear strains, there is a tendency for the soil skeleton to contract due to grain rearrangements. For larger shear strains, the soil skeleton may dilate if the soil is dense, as a result of grains riding over each other. A dilation strain-hardening table is used to model this non-monotonic behavior. For the Cysoil model, the shear-hardening flow rule has the form

$$\dot{e}^p = \dot{\gamma}^p \sin \psi_m \quad (2.265)$$

where  $\psi_m$  is the (mobilized) dilation angle.

Several different laws are available in the literature to characterize  $\psi_m$ . For the purpose of the present illustration, we use an equation based on Rowe stress-dilatancy theory (1962). According to this theory, there is a constant-volume stress ratio,  $\phi_{cv}$ , below which the material contracts (i.e. for  $\phi_m < \phi_{cv}$ ), while for higher stress ratios (i.e. for  $\phi_m > \phi_{cv}$ ), the material dilates. The equation has the form

$$\sin \psi_m = \frac{\sin \phi_m - \sin \phi_{cv}}{1 - \sin \phi_m \sin \phi_{cv}} \quad (2.266)$$

where

$$\sin \phi_{cv} = \frac{\sin \phi_f - \sin \psi_f}{1 - \sin \phi_f \sin \psi_f} \quad (2.267)$$

and  $\phi_f$  and  $\psi_f$  are ultimate (known) values of friction and dilation, respectively.

A table of dilation value versus plastic shear strain is produced for input in *FLAC*, based on the last two equations and the assumed relation between  $\phi_m$  and  $\gamma^p$  reported in [Eq. \(2.264\)](#).

#### 2.4.9.4 Implementation Procedure

Note that the parameters involved in the selected shear and volumetric hardening laws are not all independent: they must be chosen, consistent with the model assumptions. One assumption is that the ratio  $K^e / G^e$  be constant, and equal to the ratio of input upper bound values  $K$  and  $G$ . Assuming that the reference pressure is the same in [Eq. \(2.258\)](#) and [\(2.261\)](#), it follows that the exponent  $m$  should be the same in both laws. Also, we must have:

$$\frac{K}{G} = \frac{(1 + R)K_{ref}^{iso}}{G_{ref}^e} \quad (2.268)$$

Thus, the parameter  $R$  should be consistent with the choice for  $K_{ref}^{iso}$  and  $G_{ref}^e$  (assuming these were selected independently). The consistency condition gives:

$$R = \frac{K}{G} \frac{G_{ref}^e}{K_{ref}^{iso}} - 1 \quad (2.269)$$

Obviously, the derived value for  $R$  should be larger than or equal to zero.

### 2.4.9.5 Isotropic Compression Tests

Isotropic compression tests on dense, medium and loose sand are simulated using the Cysoil model with the cap-hardening law described by Eq. (2.257), input in the form of a table. The Cysoil model properties for the tests are listed in Table 2.1.

**Table 2.1** *Cysoil model properties for isotropic compr. test*

Parameter	Dense	Medium	Loose
$K_{ref}^{iso}$ (kN/m <sup>2</sup> )	40,000	30,000	20,000
$p_{ref}$ (kPa)	100	100	100
$\nu$	0.2	0.2	0.2
$m$	0.5	0.5	0.5
$R$	0.66	0.66	0.66
$\alpha$	1	1	1

The simulation is run in axisymmetric mode. The *FLAC* grid consists of three separate zones with unit dimensions, lined up along the symmetry axis. The initial stress state is isotropic in each zone; the magnitude of the confining stress is 10 kN/m<sup>2</sup>. The sand is normally consolidated for the tests (the initial cap pressure is equal to 10 kN/m<sup>2</sup>). The input values of bulk and shear modulus are set to high values, consistent with the given Poisson's ratio,  $\nu$ , listed in Table 2.1. (These input values are used as the upper bound for tangent bulk and shear elastic modulus calculated by the code). The cap behavior is assigned using a different table for each zone, consistent with the formula (Eq. (2.257)), and the data in Table 2.1. The base of the zones is fixed in the axial ( $y$ -) direction, confining velocities of magnitude  $10^{-6}$  m/step are applied at the top and lateral sides of the zone for a total of 2500 steps, five unloading/reloading excursions are also included.

A plot of vertical (axial) stress versus axial strain for the test is shown for dense, medium and loose soil cases in Figure 2.40. The plot shows the power law and stiffer behavior achieved by the denser soil, expected from the model. A plot of elastic bulk modulus versus axial strain for the test is shown in Figure 2.41. The bulk modulus is seen on the plot to remain constant during unloading/reloading; also the value is higher for higher strain levels, consistent with the dependency of the property on plastic deformation.

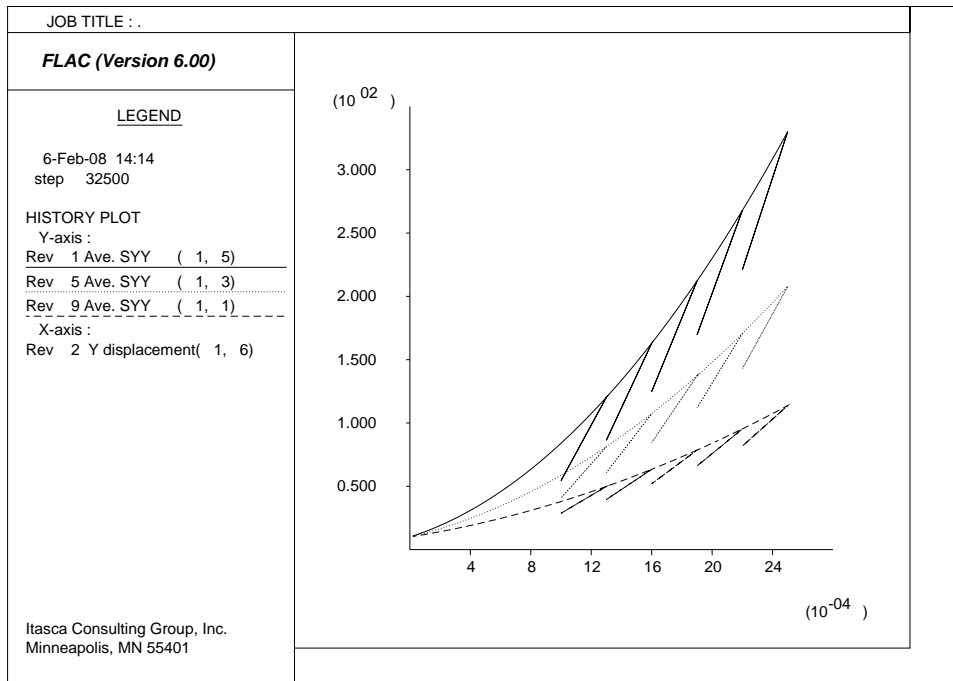


**Figure 2.40** Axial stress (in  $kN/m^2$ ) versus axial strain for dense, medium and loose sand

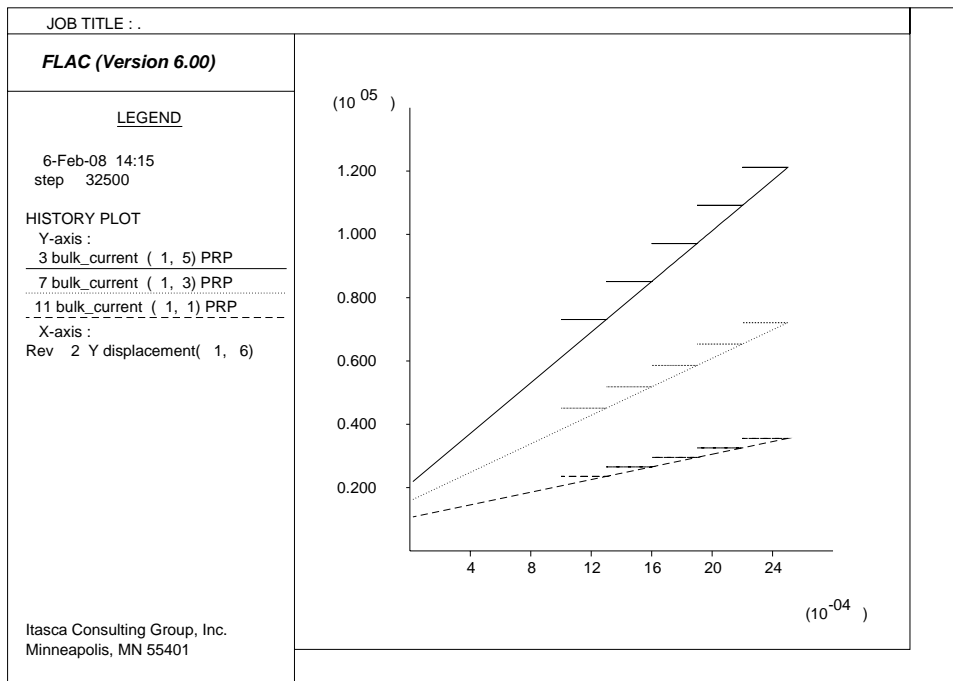


**Figure 2.41** Bulk modulus (in  $kN/m^2$ ) versus axial strain for dense, medium and loose sand

**Example 2.7 Isotropic compression tests**


---

```

def setup
; --- dense ---
  _kid  = 4e4
  _eurd = 12e4
; --- medium ---
  _kim  = 3e4
  _eurm = 9e4
; --- loose ---
  _kil  = 2e4
  _eurl = 6e4
;
  _em   = 0.5
  _Pref = 100.
  _nu   = 0.2
  _pc0  = 10.
; --- derived quantities ---
  _bulk = 1e15
  _shear= _bulk*(3.*(1.-2.*_nu))/(2.*(1.+_nu))
  _num  = 5000.
  _nt   = 1
end
setup
config axi
g 1 5
model cysoil
prop dens 1000 bulk=_bulk sh=_shear
prop friction=45. dilation=0.
prop cap_pressure=_pc0 alpha=1.
model null j=2
model null j=4
def cap_table
  _mul  = _eur/(3.*(1.-2.*_nu)*_ki) - 1.
  evpmax= 1e-2
  _de   = evpmax/float(_num)
  ratr  = (1.+_mul)/_mul
  xtable(_nt,1) = 0.0
  ytable(_nt,1) = 0.0
  coe   = 1.-_em
  _mex  = 1./coe
  _coep = _Pref*(coe*ratr*_ki/_Pref)^_mex
  loop ii (2,_num)
    xval = _de*float(ii-1)
    ytable(_nt,ii) = _coep*(xval^_mex)

```

```

        xtable(_nt,ii) = xval
    end_loop
    evp=((_pc0/_Pref)^coe)*(_mul/(1.+_mul))*_Pref/(coe*_ki)
end
; --- dense ---
set _ki=_kid _eur=_eurd _nt=1
cap_table
prop mul=_mul ev_plastic=evp cptable=_nt i=1 j=5
; --- medium ---
set _ki=_kim _eur=_eurm _nt=2
cap_table
prop mul=_mul ev_plastic=evp cptable=_nt i=1 j=3
; --- loose ---
set _ki=_kil _eur=_eurl _nt=3
cap_table
prop mul=_mul ev_plastic=evp cptable=_nt i=1 j=1
;
fix x i=2
fix y
ini sxx -10. syy -10. szz -10.
ini xvel -1e-6 i=2
ini yvel -1e-6 j=2
ini yvel -1e-6 j=4
ini yvel -1e-6 j=6
;
hist ns 20
hist syy i=1 j=5
hist ydis i=1 j=6
hist bulk_current i=1 j=5
hist shear_current i=1 j=5
;
hist syy i=1 j=3
hist ydis i=1 j=4
hist bulk_current i=1 j=3
hist shear_current i=1 j=3
;
hist syy i=1 j=1
hist ydis i=1 j=2
hist bulk_current i=1 j=1
hist shear_current i=1 j=1
;
def trip
    loop i (1,5)
        command
            ini yv -1e-6 j=2
            ini xv -1e-6 i=2

```

```

ini yv -1e-6 j=4
ini xv -1e-6 i=4
ini yv -1e-6 j=6
ini xv -1e-6 i=6
step 300
ini xv mul -.1 yv mul -.1
step 3000
ini xv mul -1. yv mul -1.
step 3000
end_command
end_loop
end
step 1000
trip
save isocmp.sav

```

---

#### 2.4.9.6 Oedometer Tests

Oedometer test simulations are carried out for different values of the parameter  $\alpha$ , to evaluate the impact of the cap aspect ratio on confining stress, when yielding occurs on the cap. The values of  $\alpha$  considered for the tests are 0.5, 1 and  $10^{20}$  (i.e. a value very large compared to 1, in which case the behavior of the double-yield model is recovered).

We use the same setup and properties (apart from  $\alpha$ ) as in the previous example, except in this case, the simulations are run in plane strain, with fixed lateral boundaries to simulate oedometer test conditions. Friction is assigned a large value to prevent shear yielding. The ratio,  $K_0$ , of confining stress to vertical stress,  $\sigma_{xx} / \sigma_{yy}$ , is plotted versus axial strain for dense, medium and loose sand in two figures below: [Figure 2.42](#) compares predictions for  $\alpha = 0.5$  and  $\alpha$ , large (double-yield model), and [Figure 2.43](#) shows plots for  $\alpha = 1.0$  and  $\alpha$ , large (double-yield model).

The results of the oedometer simulations show that, with the given properties, a higher value of  $K_0$  is achieved for the Cysoil model, compared to the double-yield model, and for all tests, the lower the aspect ratio of the cap, the higher the  $K_0$  that is achieved. Also, dense, medium and loose sands converge to the same ultimate  $K_0$  value as deformation takes place, and they do so at a faster deformation rate for the Cysoil model, compared to the double-yield model.

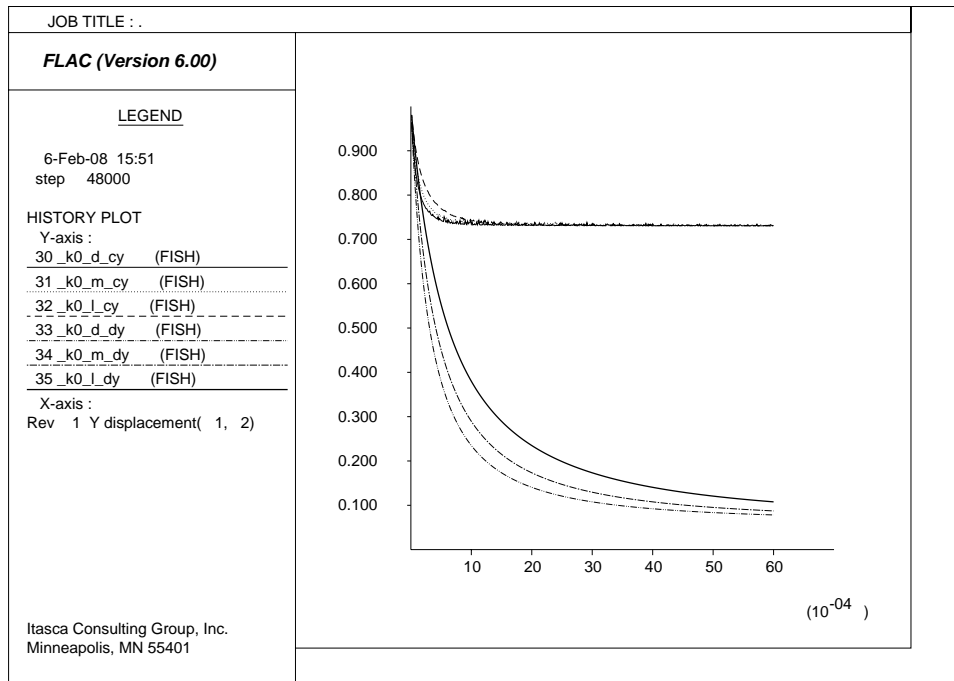


**Figure 2.42**  $K_0$  versus axial strain for dense, medium and loose sand —  $\alpha = 0.5$  (top) and double-yield model (bottom)

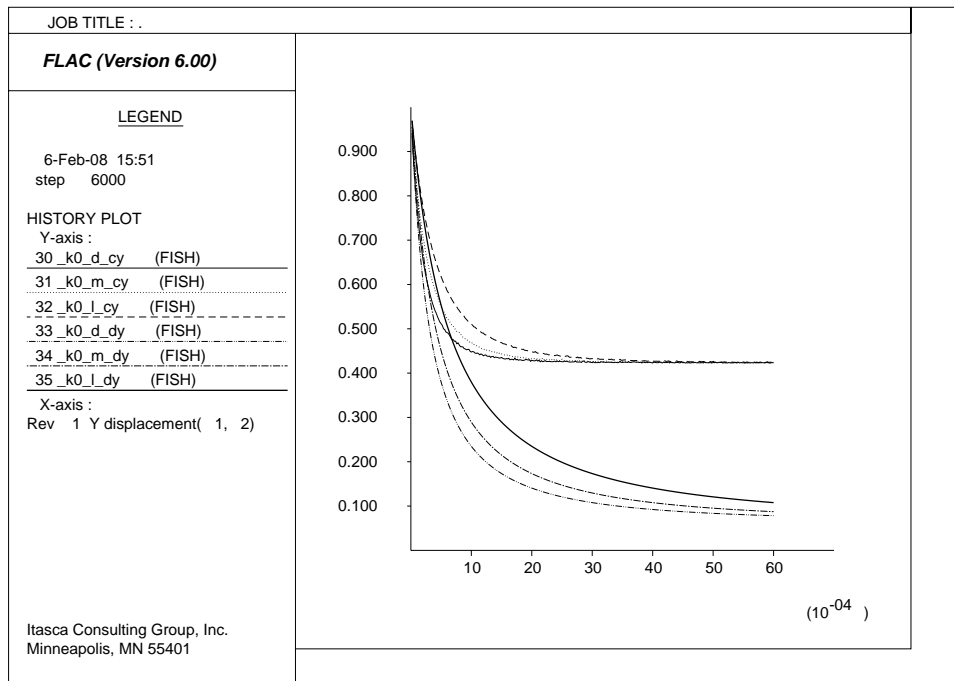


**Figure 2.43**  $K_0$  versus axial strain for dense, medium and loose sand —  $\alpha = 1.0$  (top) and double-yield model (bottom)

**Example 2.8 Oedometer tests**


---

```

def setup
  _alpha = 0.5 ;1.0 ;1e20
; --- dense ---
  _kid   = 4e4
  _eurd  = 12e4
; --- medium ---
  _kim   = 3e4
  _eurm  = 9e4
; --- loose ---
  _kil   = 2e4
  _eurl  = 6e4
;
  _em    = 0.5
  _Pref  = 100.
  _nu    = 0.2
  _pc0   = 10.
  _fric  = 89.
; --- derived quantities ---
  _bulk  = 1e15
  _shear = _bulk*(3.*(1.-2.*_nu))/(2.*(1.+_nu))
  _bc    = _bulk/1e12
  _sc    = _shear/1e12
  a12    = 2.*_alpha*_alpha/9.
  _k0    = (1.-a12)/(1.+2.*a12)
  _num   = 5000.
  _nt    = 1
end
setup
g 3 5
model cysoil                                i=1
prop dens 1000 bulk=_bulk sh=_shear i=1
prop friction=_fric dilation=0.             i=1
prop cap_pressure=_pc0 alpha=_alpha i=1
prop bulk_current=_bc shear_current=_sc i=1
model dy                                      i=3
prop dens 1000 bulk=_bulk sh=_shear i=3
prop friction=_fric dilation=0.             i=3
prop cap_pressure=_pc0                      i=3
model null i=2
model null j=2
model null j=4
def cap_table
  _mul  = _eur/(3.*(1.-2.*_nu)*_ki) - 1.

```

```

evpmax= 1e-2
_de   = evpmax/float(_num)
ratr  = (1.+_mul)/_mul
xtable(_nt,1) = 0.0
ytable(_nt,1) = 0.0
coe   = 1.-_em
_mex  = 1./coe
_coep = _Pref*(coe*ratr*_ki/_Pref)^_mex
loop ii (2,_num)
  xval = _de*float(ii-1)
  ytable(_nt,ii) = _coep*(xval^_mex)
  xtable(_nt,ii) = xval
end_loop
evp=((_pc0/_Pref)^coe)*(_mul/(1.+_mul))*_Pref/(coe*_ki)
end
; --- dense ---
set _ki=_kid _eur=_eurd _nt=1
cap_table
prop mul=_mul ev_plastic=evp cptable=_nt j=5
; --- medium ---
set _ki=_kim _eur=_eurm _nt=2
cap_table
prop mul=_mul ev_plastic=evp cptable=_nt j=3
; --- loose ---
set _ki=_kil _eur=_eurl _nt=3
cap_table
prop mul=_mul ev_plastic=evp cptable=_nt j=1
fix x y
ini sxx -10. syy -10. szz -10.
ini yvel -0.125e-6 j=2
ini yvel -0.125e-6 j=4
ini yvel -0.125e-6 j=6
hist ns 100
hist 1 ydis i=1 j=2
hist 2 syy i=1 j=5
hist 3 sxx i=1 j=5
hist 4 bulk_current i=1 j=5
hist 5 shear_current i=1 j=5
hist 6 syy i=3 j=5
hist 7 sxx i=3 j=5
hist 8 bulk i=3 j=5
hist 9 shear i=3 j=5
hist 10 syy i=1 j=3
hist 11 sxx i=1 j=3
hist 12 bulk_current i=1 j=3
hist 13 shear_current i=1 j=3

```

```
hist 14 syy i=3 j=3
hist 15 sxx i=3 j=3
hist 16 bulk_current i=1 j=3
hist 17 shear_current i=1 j=3
hist 18 syy i=1 j=1
hist 19 sxx i=1 j=1
hist 20 bulk_current i=1 j=1
hist 21 shear_current i=1 j=1
hist 22 syy i=3 j=1
hist 23 sxx i=3 j=1
hist 24 bulk_current i=1 j=1
hist 25 shear_current i=1 j=1
def _k0_d.cy
  _k0_d.cy=sxx(1,5)/syy(1,5)
  _k0_d.dy=sxx(3,5)/syy(3,5)
  _k0_m.cy=sxx(1,3)/syy(1,3)
  _k0_m.dy=sxx(3,3)/syy(3,3)
  _k0_l.cy=sxx(1,1)/syy(1,1)
  _k0_l.dy=sxx(3,1)/syy(3,1)
end
hist 30 _k0_d.cy
hist 31 _k0_m.cy
hist 32 _k0_l.cy
hist 33 _k0_d.dy
hist 34 _k0_m.dy
hist 35 _k0_l.dy
hist 36 _k0
step 48000
save oedol.sav
ret
```

---

#### 2.4.9.7 Drained Triaxial Tests - Constant Dilation

Triaxial tests on dense, medium and loose sand are simulated using the Cysoil model with the friction-hardening law described in Eq. (2.263) — input in the form of tables. The model properties are listed in Table 2.2 below. The cap pressure is assigned a value very large compared to the stress level reached in the simulations in order to prevent yielding on the cap. The cap  $\alpha$  is 1.

The simulation is run in axisymmetric mode. The *FLAC* grid consists of one zone with unit dimensions. The initial stress state is isotropic, with mean pressure equal to 100 kN/m<sup>2</sup>. The lateral pressure is kept constant during the test, the base of the model is fixed in the axial (*y*-) direction, and an axial velocity of 10<sup>-6</sup> m/step is applied at the top of the model for a total of 5000 steps. In addition, three unloading/reloading excursions are performed.

**Table 2.2** *Cysoil model properties for triaxial test*

Parameter	Dense	Medium	Loose
$G_{ref}^e$ (kN/m <sup>2</sup> )	50,000	37,500	25,000
$p_{ref}$ (kPa)	100	100	100
$\nu$	0.2	0.2	0.2
$m$	1	1	1
$\phi_f$ (degrees)	40	35	30
$\psi_f$ (degrees)	10	5	0
$R_f$	0.9	0.9	0.9
$\beta$	0.35	0.35	0.35

A plot of deviatoric stress versus axial strain for the test is shown in Figure 2.44, for dense, medium and loose sand cases. The plot shows the hyperbolic behavior expected from the model, and the higher failure level achieved by the denser soil. Three unloading/reloading excursions, also shown on the figure, illustrate the model capabilities. The plot of volumetric strain versus axial strain for the tests is shown in Figure 2.45. The volumetric behavior is monotonic in the plot, the dilatant behavior of the dense sand is clearly shown.

Example 2.9 lists the data file for the triaxial test on dense sand. Test results for all three cases are written to tables. Example 2.10 lists the data file which creates plots in Figures 2.44 and 2.45 to compare the three cases.

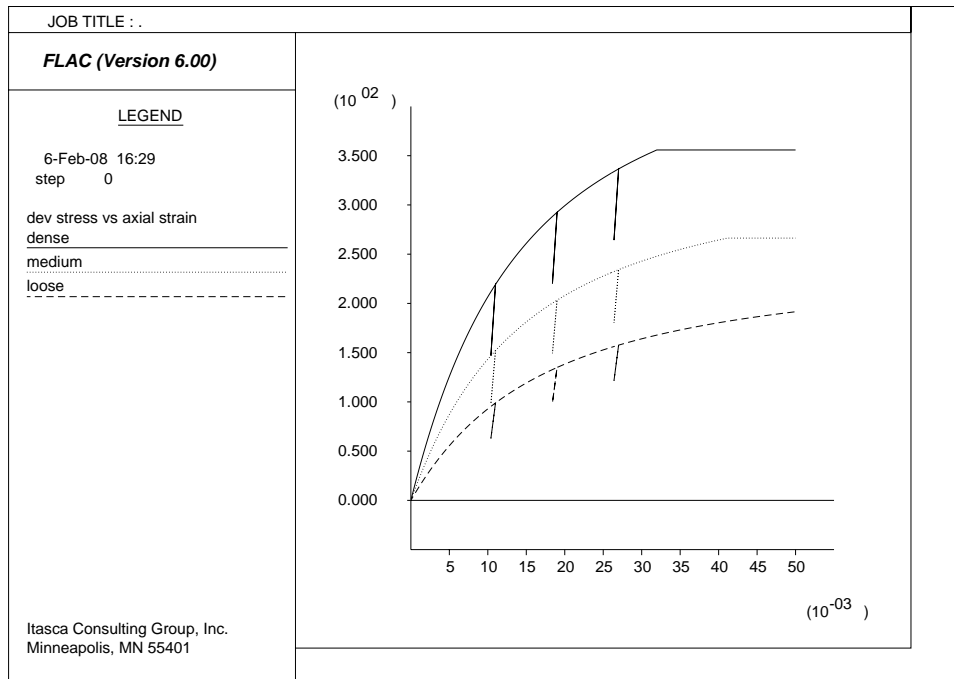


**Figure 2.44**  $|\sigma_1 - \sigma_3|$  (in  $\text{kN/m}^2$ ) versus axial strain for dense, medium and loose sand — constant dilation

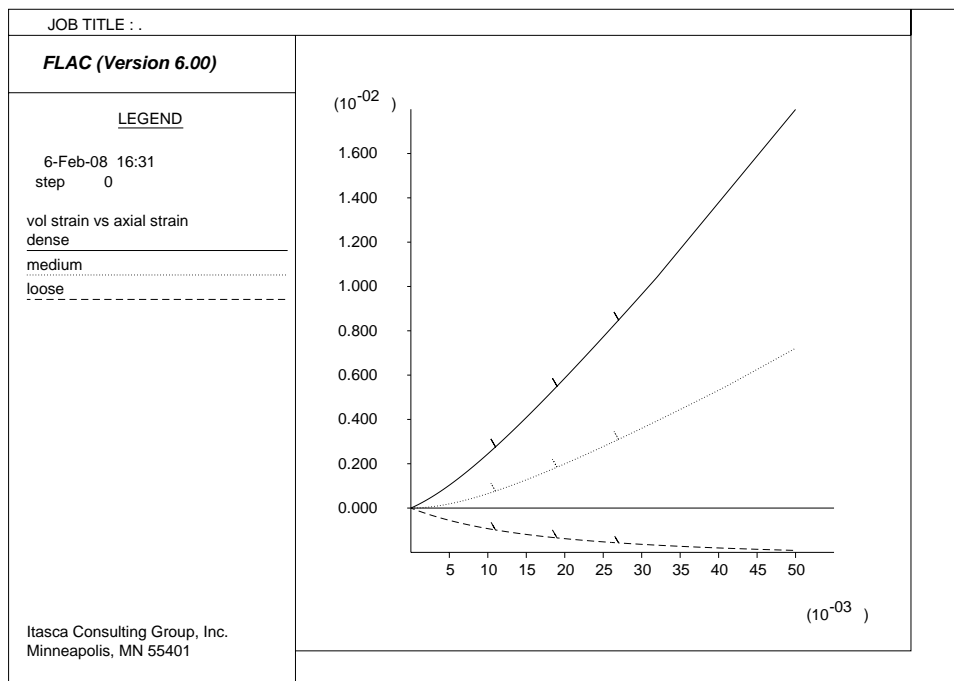


**Figure 2.45** Volumetric strain versus axial strain for dense, medium and loose sand — constant dilation

**Example 2.9 Triaxial tests — dense sand case (constant dilation)**


---

```

new
title
  Drained triaxial test - dense cysoil
def setup
  _nu    = 0.2
  _kref  = 120e3/(3.*(1.-2.*_nu))      ; reference tangent bulk mod
  _gref  = 120e3/(2.*(1.+_nu))        ; reference tangent shear mod
  _Pa    = 100.                        ; reference pressure
  _fri_u = 40.                         ; ultimate friction
  _fric  = 0.0                         ; initial friction
  _dil   = 10.0                        ; dilation
  _al    = 1.0                         ; alpha for cap
  _Rf    = 0.90                        ; failure ratio Rf
  _beta  = 0.35
  _yv    = -1e-6 ; -1e-9
  _p0    = 100.
; --- derived quantities ---
  _mp0   = -_p0
  _g      = _gref*_p0/_Pa              ; elastic shear modulus
  _k      = _kref*_p0/_Pa              ; elastic bulk modulus
  _sinu   = sin(_fri_u*degrad)
;
; --- friction hardening table ---
  _Gi    = _beta*( _gref/_Pa)
  _num   = 200
  loop ii (1,_num)
    _phic = (_fri_u/float(_num))*float(ii-1)
    sval  = sin(_phic*degrad)
    _coe  = _sinu/_Rf
    xval  = (_coe/(1.-sval/_coe)-_coe)/_Gi
    ytable(1,ii) = _phic
    xtable(1,ii) = xval
  end_loop
  ytable(1,_num+1) = _phic
  xtable(1,_num+1) = 0.1
; (initial value of plastic shear strain)
  sval  = sin(_fric*degrad)
  _coe  = _sinu/_Rf
  _esp  = (_coe/(1.-sval/_coe)-_coe)/_Gi
end
setup
config axi extra 10
grid 1,1

```

```
model cysoil
prop dens 1000 bulk=_k shear=_g friction=_fric dilation=_dil
prop cap_pressure=1e20 alpha=_al
prop es_plastic=_esp ev_plastic=0.0
prop ftable 1
;
fix y
ini sxx _mp0 syy _mp0 szz _mp0
apply sxx _mp0 i=2
ini yvel _yv j 2
;
hist 1 cy_q i 1 j 1
hist 2 cy_p i 1 j 1
hist 3 syy i 1 j 1
hist 4 sxx i 1 j 1
hist 5 szz i 1 j 1
hist 6 ydisp i 1 j 2
hist 7 cap_pressure i 1 j 1
hist 8 es_plastic i 1 j 1
hist 9 ev_plastic i 1 j 1
hist 10 et_plastic i 1 j 1
hist 11 friction_mob i 1 j 1
hist 12 dilation_mob i 1 j 1
hist 13 vsi i 1 j 1
hist 14 bulk_current i 1 j 1
hist 15 shear_current i 1 j 1
hist nstep 50
def trip
  loop i (1,3)
    command
      ini yv -1e-6 j=2
      step 8000
      ini yv mul -.1 j=2
      step 6000
      ini yv mul -1. j=2
      step 6000
    end_command
  end_loop
end
step 3000
trip
ini yv -1e-6 j=2
step 23000
;
his write 1 vs -6 tab 10
his write 13 vs -6 tab 11
```

```
;
def setupd
  name = 'dense-ds'
  nameoflog = name+'.log'
  tab_num=10
end
def setupv
  name = 'dense-ev'
  nameoflog = name+'.log'
  tab_num=11
end
def log_it
  nump=table_size(tab_num)
  command
    set log @nameoflog
    set log on
  end_command
  oo=out(name)
  oo=out(string(nump)+' '+string(0.0))
  loop ll (1,nump)
    xl = xtable(tab_num,ll)
    yl = ytable(tab_num,ll)
    oo=out(string(xl)+' '+string(yl))
  end_loop
  command
    set log off
  end_command
end
setupd
log_it
setupv
log_it
save td.sav
ret
```

---

**Example 2.10 Triaxial tests — compare results**

---

```
new
title
  Drained triaxial test - cysoil
table 10 read dense-ds.log
table 11 read dense-ev.log
table 20 read medium-ds.log
table 21 read medium-ev.log
table 30 read loose-ds.log
table 31 read loose-ev.log
label table 10
dense ds
label table 11
dense ev
label table 20
medium ds
label table 21
medium ev
label table 30
loose ds
label table 31
loose ev
plot hold table 10 lin 20 lin 30 lin
plot hold table 11 lin 21 lin 31 lin
set plot jpg color
set out triax-ds.jpg
plot pen table 10 lin 20 lin 30 lin
set out triax-ev.jpg
plot pen table 11 lin 21 lin 31 lin
save triax.sav
ret
```

---

### 2.4.9.8 Drained Triaxial Tests - Dilation Hardening

The triaxial test simulations with friction hardening in [Section 2.4.9.7](#) are repeated, this time using in addition, a dilation hardening table as described by [Eq. \(2.265\)](#). Initial dilation is zero, and the ultimate value of dilation is listed in [Table 2.2](#). [Example 2.11](#) lists the data file for the triaxial test on dense sand including dilation hardening. The results of all three cases are compared, as before, by writing the results to tables and creating plots using the command file listed in [Example 2.10](#).

The simulation results of deviatoric stress and volumetric strain versus axial strain are plotted in [Figures 2.46](#) and [2.47](#), respectively. The non-monotonic volumetric behavior is apparent in the second plot: all soil types do compact initially, and the denser soil is shown to dilate upon further shearing.

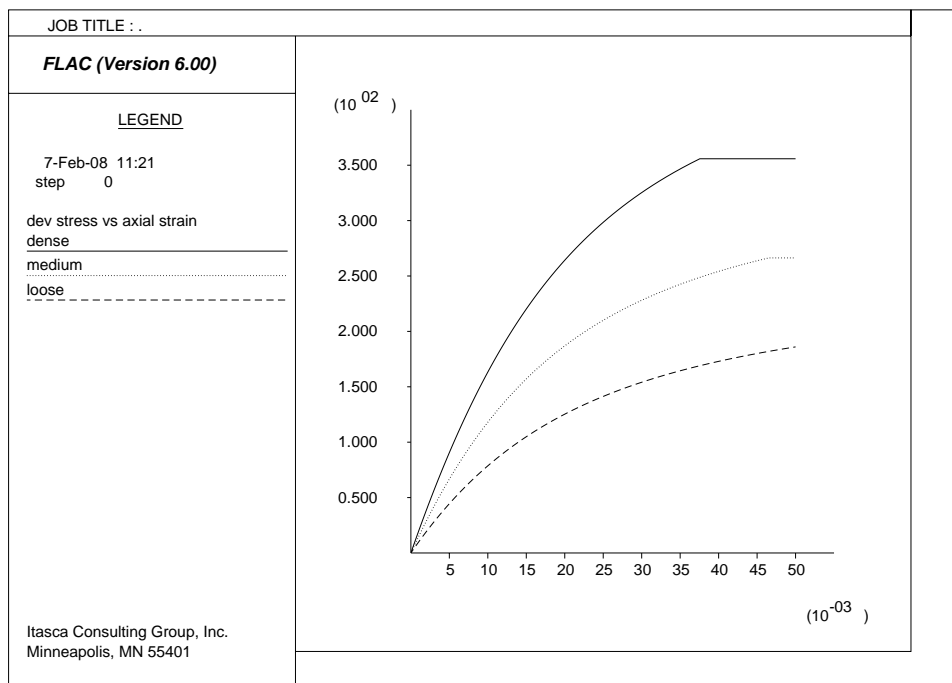


**Figure 2.46**  $|\sigma_1 - \sigma_3|$  (in  $\text{kN/m}^2$ ) versus axial strain for dense, medium and loose sand — dilation hardening

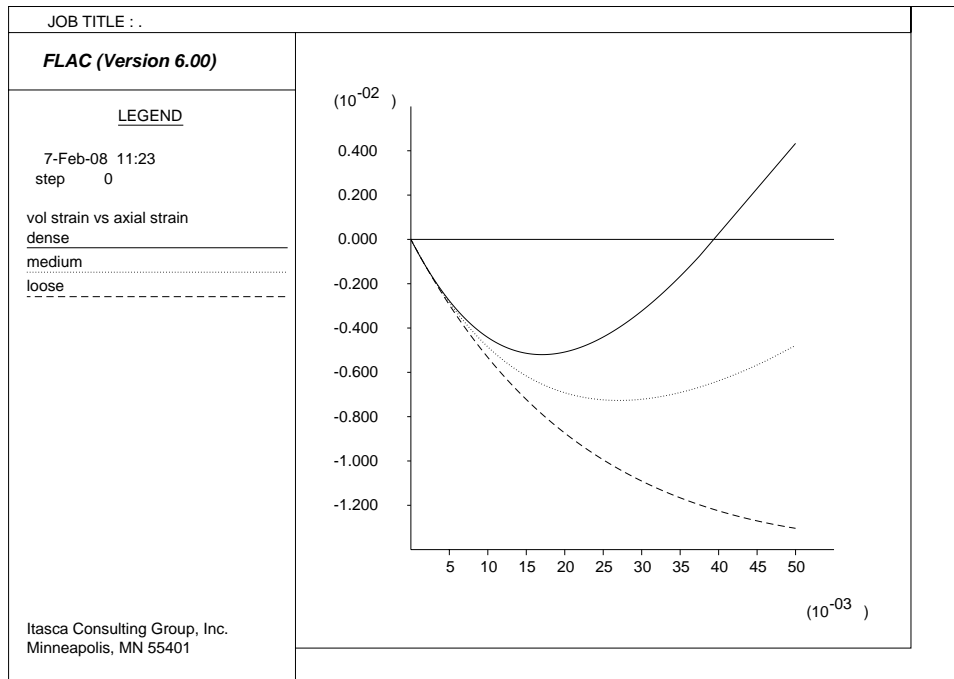


**Figure 2.47** Volumetric strain versus axial strain for dense, medium and loose sand — dilation hardening

**Example 2.11** Triaxial tests — dense sand case (dilation hardening)

```

new
title
  Drained triaxial test - dense cysoil
def setup
  _nu = 0.2
  _kref = 120e3/(3.*(1.-2.*_nu)) ; reference tangent bulk mod
  _gref = 120e3/(2.*(1.+_nu)) ; reference tangent shear mod
  _Pa = 100. ; reference pressure
  _fri0 = 40. ; ultimate friction
  _fric = 0.0 ; initial friction
  _dil0 = 10.0 ; ultimate dilation
  _Rf = 0.90 ; failure ratio Rf
  _beta = 0.35
  _yv = -1e-6
  _p0 = 100.
  _cp = 1e20 ; cap
; --- derived quantities ---
  _mp0 = -_p0
  _g = _gref*_p0/_Pa ; elastic shear modulus
  _k = _kref*_p0/_Pa ; elastic bulk modulus

```

```

_sinu = sin(_frii*degrad)
_sin  = sin(_fric*degrad)
_sind = sin(_dilu*degrad)
_sincv = (_sinu-_sind)/(1.-_sinu*_sind)
_fricv = 180.0*atan(sqrt(_sincv^2/(1-_sincv^2)))/pi
_al    = 1.
; --- friction hardening and dilation tables ---
_Gi    = _beta*(_gref/_Pa)
_num   = 200
loop ii (1,_num)
  _phic = (_frii/float(_num))*float(ii-1)
  sval  = sin(_phic*degrad)
  _coe  = _sinu/_Rf
  xval  = (_coe/(1.-sval/_coe)-_coe)/_Gi
  ytable(1,ii) = _phic
  xtable(1,ii) = xval
  sinpsi = (sval-_sincv)/(1.-sval*_sincv)
  _psic  = 180.0*atan(sqrt(sinpsi^2/(1-sinpsi^2)))/pi
  if sinpsi < 0.0 then
    _psic = -_psic
  end_if
  ytable(2,ii) = min(_psic,_dilu)
  xtable(2,ii) = xval
end_loop
ytable(1,_num+1) = _phic
xtable(1,_num+1) = 0.1
ytable(2,_num+1) = _psic
xtable(2,_num+1) = 0.1
; (initial value of plastic shear strain)
sval  = sin(_fric*degrad)
_coe  = _sinu/_Rf
_esp  = (_coe/(1.-sval/_coe)-_coe)/_Gi
end
setup
config axi extra 10
grid 1,1
model cysoil
prop dens 1000 bulk=_k shear=_g cohesion=0. friction=_fric
prop dilation=0.
prop tension=1.0E10 cap_pressure=_cp alpha=_al
prop es_plastic=_esp ev_plastic=0.0
prop ftable 1
prop dtable 2
;
fix y
ini sxx _mp0 syy _mp0 szz _mp0

```

```
apply sxx _mp0 i=2
ini yvel _yv j 2
;
hist 1 cy_q i 1 j 1
hist 2 cy_p i 1 j 1
hist 3 syy i 1 j 1
hist 4 sxx i 1 j 1
hist 5 szz i 1 j 1
hist 6 ydisp i 1 j 2
hist 7 cap_pressure i 1 j 1
hist 8 es_plastic i 1 j 1
hist 9 ev_plastic i 1 j 1
hist 10 et_plastic i 1 j 1
hist 11 friction_mob i 1 j 1
hist 12 dilation_mob i 1 j 1
hist 13 vsi i 1 j 1
hist 14 bulk_current i 1 j 1
hist 15 shear_current i 1 j 1
;
hist nstep 50
step 50000
;
his write 1 vs -6 tab 10
his write 13 vs -6 tab 11
;
def setupd
  name = 'dense-ds'
  nameoflog = name+'.log'
  tab_num=10
end
def setupv
  name = 'dense-ev'
  nameoflog = name+'.log'
  tab_num=11
end
def log_it
  nump=table_size(tab_num)
  command
    set log @nameoflog
    set log on
  end_command
  oo=out(name)
  oo=out(string(nump)+' '+string(0.0))
  loop ll (1,nump)
    xl = xtable(tab_num,ll)
    yl = ytable(tab_num,ll)
```

```
        oo=out(string(xl)+' '+string(yl))
    end_loop
command
    set log off
end_command
end
setupd
log_it
setupv
log_it
save td.sav
ret
```

---

2.4.9.9 Undrained Triaxial Tests

Tests similar to those in Sections 2.4.9.7 and 2.4.9.8 are repeated, but this time under undrained conditions. The model setup and properties are the same as those used in the previous examples. In addition, the groundwater flow configuration is selected, with flow turned off. Porosity is 0.3, and the fluid bulk modulus is 2000 kPa for the runs.

The undrained simulation results for deviatoric stress and volumetric strain versus axial strain are plotted in Figures 2.48 and 2.49, respectively. A softening stress-strain response is observed for the loose soil in Figure 2.48. Also, while the excess pore pressure is indicated in Figure 2.49 to rise initially for all soils, for the medium and dense soils, it is shown to decrease upon further shearing as a result of dilation taking place.

Example 2.12 lists the data file for the dense soil case. All three cases are compared in Figures 2.48 and 2.49 by loading the table results as described in Example 2.10.

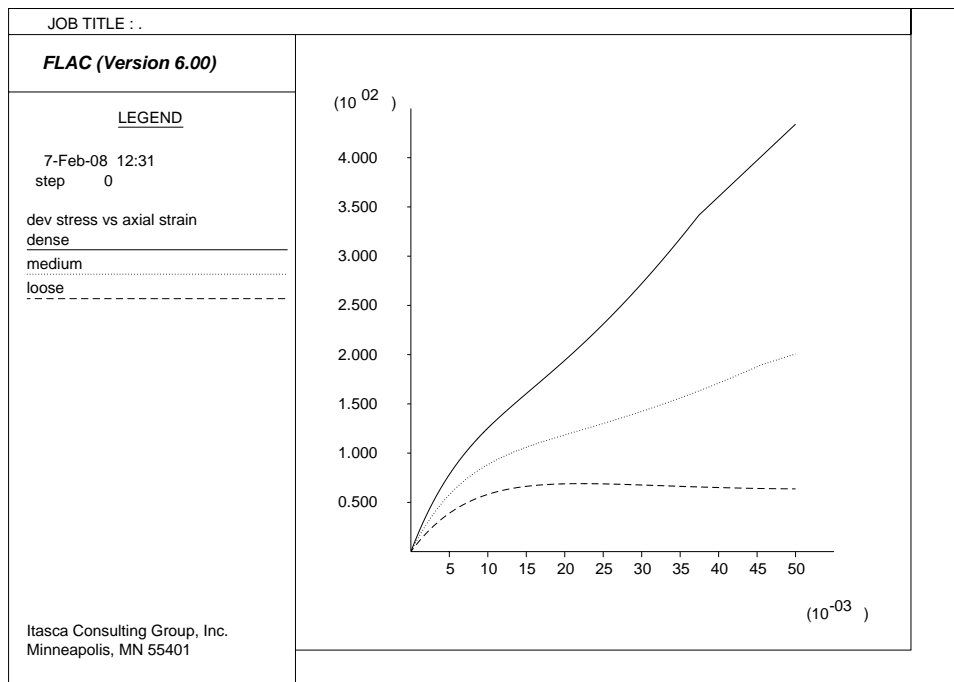
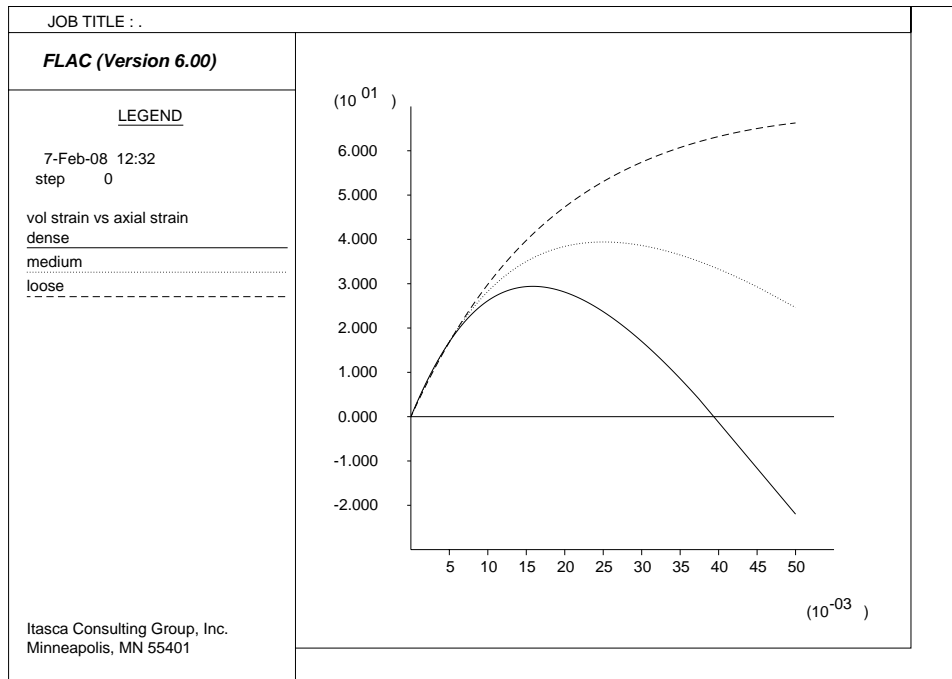


Figure 2.48  $|\sigma_1 - \sigma_3|$  (in  $kN/m^2$ ) versus axial strain for dense, medium and loose sand — undrained triaxial tests



**Figure 2.49** Volumetric strain versus axial strain for dense, medium and loose sand — undrained triaxial tests

**Example 2.12** Triaxial tests — dense sand case (undrained)

```

new
title
  Undrained triaxial test - dense cysoil
def setup
  _nu = 0.2
  _kref = 120e3/(3.*(1.-2.*_nu)) ; reference tangent bulk mod
  _gref = 120e3/(2.*(1.+_nu)) ; reference tangent shear mod
  _Pa = 100. ; reference pressure
  _fri_u = 40. ; ultimate friction
  _fric = 0.0 ; initial friction
  _dil_u = 10.0 ; ultimate dilation
  _Rf = 0.90 ; failure ratio Rf
  _beta = 0.35
  _yv = -1e-6
  _p0 = 100.
  _cp = 1e20 ; cap
; --- derived quantities ---
  _mp0 = -_p0
  _g = _gref*_p0/_Pa ; elastic shear modulus
  _k = _kref*_p0/_Pa ; elastic bulk modulus

```

```

_sinu = sin(_frii*degrad)
_sin  = sin(_fric*degrad)
_sind = sin(_dilu*degrad)
_sincv = (_sinu-_sind)/(1.-_sinu*_sind)
_fricv = 180.0*atan(sqrt(_sincv^2/(1-_sincv^2)))/pi
_al    = 1.
; --- friction hardening and dilation tables ---
_Gi    = _beta*(_gref/_Pa)
_num   = 200
loop ii (1,_num)
  _phic = (_frii/float(_num))*float(ii-1)
  sval  = sin(_phic*degrad)
  _coe  = _sinu/_Rf
  xval  = (_coe/(1.-sval/_coe)-_coe)/_Gi
  ytable(1,ii) = _phic
  xtable(1,ii) = xval
  sinpsi = (sval-_sincv)/(1.-sval*_sincv)
  _psic  = 180.0*atan(sqrt(sinpsi^2/(1-sinpsi^2)))/pi
  if sinpsi < 0.0 then
    _psic = -_psic
  end_if
  ytable(2,ii) = min(_psic,_dilu)
  xtable(2,ii) = xval
end_loop
ytable(1,_num+1) = _phic
xtable(1,_num+1) = 0.1
ytable(2,_num+1) = _psic
xtable(2,_num+1) = 0.1
; (initial value of plastic shear strain)
sval  = sin(_fric*degrad)
_coe  = _sinu/_Rf
_esp  = (_coe/(1.-sval/_coe)-_coe)/_Gi
end
setup
config gw axi extra 10
grid 1,1
model cysoil
prop dens 1000 bulk=_k shear=_g cohesion=0. friction=_fric
prop dilation=0.
prop tension=1.0E10 cap_pressure=_cp alpha=_al
prop es_plastic=_esp ev_plastic=0.0
prop ftable 1
prop dtable 2

; --- fluid part ---
prop poros 0.3

```

```

ini ftens -1e20
ini fmod 2e3
set flow off
set force 0 sratio 1e-5
;
fix y
ini sxx _mp0 syy _mp0 szz _mp0
apply sxx _mp0 i=2
ini yvel _yv j 2
;
hist 1 cy_q i 1 j 1
hist 2 cy_p i 1 j 1
hist 3 syy i 1 j 1
hist 4 sxx i 1 j 1
hist 5 szz i 1 j 1
hist 6 ydisp i 1 j 2
hist 7 cap_pressure i 1 j 1
hist 8 es_plastic i 1 j 1
hist 9 ev_plastic i 1 j 1
hist 10 et_plastic i 1 j 1
hist 11 friction_mob i 1 j 1
hist 12 dilation_mob i 1 j 1
hist 13 vsi i 1 j 1
hist 14 bulk_current i 1 j 1
hist 15 shear_current i 1 j 1
hist 20 pp i 1 j 1
hist nstep 50
step 50000
plot hold his 1 vs -6
;plot hold his 12 vs -6
plot hold his 13 vs -6
plot hold his 20 vs -6
;
his write 1 vs -6 tab 10
his write 20 vs -6 tab 11
;
def setupd
  name = 'dense-uds'
  nameoflog = name+'.log'
  tab_num=10
end
def setupv
  name = 'dense-pp'
  nameoflog = name+'.log'
  tab_num=11
end

```

```
def log_it
  nump=table_size(tab_num)
  command
    set log @nameoflog
    set log on
  end_command
  oo=out(name)
  oo=out(string(nump)+' '+string(0.0))
  loop ll (1,nump)
    xl = xtable(tab_num,ll)
    yl = ytable(tab_num,ll)
    oo=out(string(xl)+' '+string(yl))
  end_loop
  command
    set log off
  end_command
end
setupd
log_it
setupv
log_it
save utd.sav
ret
```

---

## 2.5 References

- Amadei, B. *The Influence of Rock Anisotropy on Measurement of Stresses In Situ*. Ph.D. Thesis, University of California, Berkeley, January, 1982.
- Boukpeti, N. *Modeling Static Liquefaction in Granular Deposits*. Ph.D. Thesis, University of Minnesota, 2001.
- Britto, A. M., and M. J. Gunn. *Critical State Soil Mechanics via Finite Elements*. Chichester U.K.: Ellis Horwood Ltd., 1987.
- Byrne, P.M., Park, S.S. and Beaty, M. “Seismic Liquefaction: Centrifuge and Numerical Modeling,” in *FLAC and Numerical Modeling in Geomechanics - 2003; Proc. of the 3rd International FLAC Symposium*, pp 321-331. 21-24 October 2003, Sudbury, Ontario, Canada: Lisse: A.A. Balkema, 2003.
- Carter, T. G., J. L. Carvalho and G. Swan. “Towards the Practical Application of Ground Reaction Curves,” in *Innovative Mine Design for the 21st Century (Proceedings of the International Congress on Mine Design — Kingston, Ontario, Canada — August 1993)*, pp. 151-171. W. F. Bawden and J. F. Archibald, Eds. Rotterdam: A. A. Balkema, 1993.
- Chen, W. F., and D. J. Han. *Plasticity for Structural Engineers*. New York: Springer-Verlag, 1988.
- Cundall, P., C. Carranza-Torres and R. Hart. “A New Constitutive Model Based on the Hoek-Brown Criterion,” in *FLAC and Numerical Modeling in Geomechanics — 2003 (Proceedings of the 3rd International FLAC Symposium, Sudbury, Ontario, Canada, October 2003)*, pp. 17-25. R. Brummer, et al., Eds. Lisse: Balkema, 2003.
- Davis, R. O. and A. P. S. Selvadurai. *Plasticity and geomechanics*, Cambridge, 2002.
- Drescher, A. *Analytical Methods in Bin-Load Analysis*. Amsterdam: Elsevier, 1991.
- Duncan, J. M., and C-Y. Chang. “Nonlinear Analysis of Stress and Strain in Soils,” *Soil Mechanics*, **96**(SM5), 1629-1653 (1970).
- Hoek, E., and E. T. Brown. “Practical Estimates of Rock Mass Strength,” *Int. J. Rock Mech. Min. Sci.*, **34**(8), 1165-1186 (1998).
- Hoek, E., and E. T. Brown. *Underground Excavations in Rock*. London: IMM, 1980.
- Hoek, E., C. Carranza-Torres and B. Corkum. “Hoek-Brown Failure Criterion — 2002 Edition,” in *Proceedings of NARMS-TAC 2002, 5th North American Rock Mechanics Symposium and 17th Tunnelling Association of Canada Conference — Toronto, Canada — July 7 to 10, 2002*. Vol. 1., pp. 267-271, R. Hammah, W. Bawden, J. Curran and M. Telesnicki, Eds. Toronto: University of Toronto Press, 2002.
- Lekhnitskii, S. G. *Theory of Elasticity of an Anisotropic Body*. Moscow: Mir Publishers, 1981.

Pan, X. D., and J. A. Hudson. "A Simplified Three Dimensional Hoek-Brown Yield Criterion," in *Rock Mechanics and Power Plants (Proceedings of the ISRM Symp.*, pp. 95-103. M. Romana, Ed. Rotterdam: A. A. Balkema, 1988.

Roscoe K. H., and J. B. Burland. "On the Generalised Stress-Strain Behavior of 'Wet Clay'," in *Engineering Plasticity*, pp. 535-609. J. Heyman and F. A. Leckie, Eds. Cambridge: Cambridge University Press, 1968.

Rowe, P.W. "The Stress-Dilatancy Relation for Static Equilibrium of an Assembly of Particles in Contact," *Proc. Roy. Soc. A.*, **269**,500-527 (1962)

Shah, S. *A Study of the Behaviour of Jointed Rock Masses*. Ph.D. Thesis, University of Toronto, 1992.

Vermeer, P. A., and R. de Borst. "Non-Associated Plasticity for Soils, Concrete and Rock," *Heron*, **29**(3), 3-64 (1984).

Wood, D. M. *Soil Behaviour and Critical State Soil Mechanics*. Cambridge: Cambridge University Press, 1990.

